The Treatment of Thin Wire and Coaxial Structures in Lossless and Lossy Media in FDTD by the Modification of Assigned Material Parameters

Chris J. Railton, Dominique L. Paul, *Member, IEEE*, and Sema Dumanli

***Abstract*—It has been shown recently that the use of modified assigned material parameters (MAMPs) within the finite-difference time-domain (FDTD) method provides a systematic, readily extensible, accurate, and efficient approach to the electromagnetic analysis of microstrip structures. In this paper, it is shown that this technique can also be applied with equal effect to lossless and lossy coaxial lines, wires in a lossy medium such as earthing grids, and more complex structures which include coaxial feeds and shorting posts. The modified parameters are calculated directly from the known asymptotic fields near the wire and do not rely on the concept of "equivalent radius." Results are given which show equal or superior performance compared to those obtained using other methods but with the added advantage of flexibility and rigor.**

***Index Terms*—Coaxial transmission lines, finite-difference time-domain (FDTD) methods, wire grids.**

I. Introduction

IT WAS SHOWN in [1] that the effects of field singularities in the region of wires and strips can be accounted for within the finite-difference time-domain (FDTD) method, by altering the permittivities and permeabilities assigned to the neighboring E- and H-field nodes. The required values for these modified assigned material parameters (MAMPs) were ascertained empirically by performing many FDTD runs on simple example structures. A mapping between the material parameters and the fringing capacitance and inductance was derived, which was then used to produce look-up tables for use in the FDTD program. In [2], it was shown that this technique could be effectively applied to more complex structures, such as a microstrip filter, in a way that reduced the dependency of the results on the choice of the mesh. In addition, the use of this technique allowed a coarser mesh to be used with equivalent accuracy. In [3], the same technique was shown to be effective for a waveguide filter containing a complex iris structure.

In [4], it was shown how, in many situations, MAMPs can be derived analytically, thus avoiding the need for the empirical look-up tables. It was demonstrated that the method was effective in the analysis of stripline, wire transmission line, microstrip, and a strip-fed microstrip patch antenna. In this paper, MAMPs are developed further and extended to enable them to be applied, with equal effectiveness, to lossless and lossy coaxial structures and to wires embedded in a lossy medium. It is demonstrated that this approach can deliver equal or superior accuracy when compared to other enhanced FDTD schemes, such as shown in [5], but with the added advantage of flexibility, extensibility, and rigor.

Manuscript received September 23, 2005; revised July 31, 2006.

C. J. Railton and D. L. Paul are with the Centre for Communications Research, University of Bristol, Bristol BS8 1UB, U.K. (e-mail: chris.railton@bristol.ac.uk; d.l.paul@bristol.ac.uk).

S. Dumanli was with the Centre for Communications Research, University of Bristol, Bristol BS8 1UB, U.K. She is now with Aselsan A S, Ankara, Turkey (e-mail: eexsd@bristol.ac.uk).

Digital Object Identifier 10.1109/TEMC.2006.884452

II. Analytical Derivation of MAMPs

The general concept of MAMPs within the FDTD method was described in detail in [4]. So, only the key steps are given here.

Consider the Maxwell's equations in the integral form.

$$\frac{\partial}{\partial t}\iint_S \varepsilon E\, dS + \iint_S \sigma E\, dS = \oint H\, dl \tag{1}$$

$$\frac{\partial}{\partial t}\iint_S \mu H\, dS = -\oint E\, dl \tag{2}$$

Applying these to an FDTD mesh in the usual way yields (3) and (4), shown at the bottom of the next page, where $\delta x, \delta y$, and δz are the cell sizes, i, j, and k are the serial numbers of the cell, $\langle a \rangle_x$ is the average of the quantity, a, along an x directed cell edge and $\langle\langle a \rangle\rangle_{xy}$ is the average of the quantity, a, over an xy cell face. The other four update equations can be obtained by rotating the coordinates. This approach is similar to that used in the finite integration technique [6], [7].

In order to complete this set of equations, it is necessary to relate the surface averages on the left-hand side of the equations to the line averages given on the right-hand side. If the fields are assumed to be constant within each cell, which is equivalent to expanding them in a set of pulse basis functions, then the two are the same and the standard FDTD update equations are obtained. However, in the vicinity of a wire or an edge, if the asymptotic field behavior is known, a more accurate relation can be obtained.

Inspection of the equations shows that the ratios of the surface averages to the line averages can be expressed as a modification to the material parameters in the cell. This leads to a particularly simple and physically meaningful result in (5) and (6), shown at the bottom of the next page.

As long as the behavior of the x component of the E field is known in the space surrounding the singularity, this

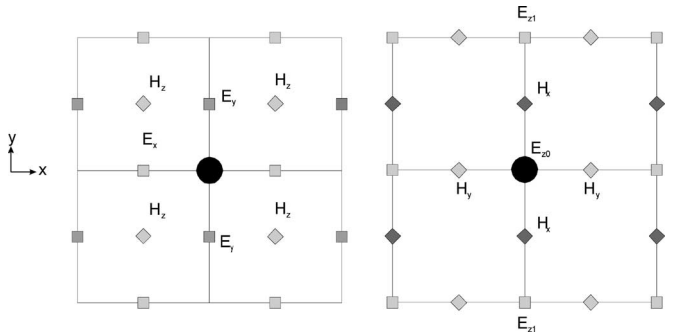

Fig. 1. Thin wire embedded in the FDTD mesh. TE plane (*left*), TM plane (*right*).

parameter is readily calculated. In the final program, only the line integrals are stored; the surface integrals are not explicitly calculated.

Treating the update equations for the magnetic fields in a similar way leads to a modified permeability parameter defined as

$$\mu_x = \frac{\langle\langle H_x \rangle\rangle_{yz}}{\langle H_x \rangle_x}. \tag{7}$$

The value of the permittivity used in the update equation for E_x is multiplied by ε_x and the value of permeability used in the update equation for H_x is multiplied by μ_x. The update equations for the other field components are treated similarly.

It is known (for example, [8]) that the singular fields around a wire located along a line of E_z nodes, as shown in Fig. 1, are given as follows:

$$E_x(x,y) \propto H_y(x,y) \propto \frac{x}{x^2+y^2} \tag{8}$$

$$E_y(x,y) \propto H_x(x,y) \propto \frac{y}{x^2+y^2} \tag{9}$$

$$E_z(x,y) \propto H_z(x,y) \propto Ln\left(\frac{\sqrt{x^2+y^2}}{a}\right) \tag{10}$$

where a is the wire radius.

The required ratios which yield the MAMPs then follow immediately:

$$\begin{aligned}\mu_y &= \frac{\langle E_x \rangle_x}{\langle\langle E_x \rangle\rangle_{yz}} = \frac{\langle\langle H_y \rangle\rangle_{xz}}{\langle H_y \rangle_y} \\ &= \frac{\delta y \int_a^{\delta x} \frac{x}{x^2+y^2} dx}{\delta x \int_{-\delta y/2}^{\delta y/2} \frac{x}{x^2+y^2} dy} \\ &= \frac{\ln\left(\frac{\delta x}{a}\right)}{2\tan^{-1}\left(\frac{\delta y}{\delta x}\right)} \frac{\delta y}{\delta x}\end{aligned} \tag{11}$$

$$\begin{aligned}\mu_x &= \frac{\langle E_y \rangle_y}{\langle\langle E_y \rangle\rangle_{xz}} = \frac{\langle\langle H_x \rangle\rangle_{yz}}{\langle H_x \rangle_x} \\ &= \frac{\delta x \int_a^{\delta y} \frac{y}{x^2+y^2} dy}{\delta y \int_{-\delta x/2}^{\delta x/2} \frac{y}{x^2+y^2} dx} \\ &= \frac{\ln\left(\frac{\delta y}{a}\right)}{2\tan^{-1}\left(\frac{\delta x}{\delta y}\right)} \frac{\delta x}{\delta y}\end{aligned} \tag{12}$$

$$\begin{aligned}\mu_z &= \frac{\langle\langle H_z \rangle\rangle_{xy}}{\langle H_z \rangle_z} \\ &= \frac{2\int_0^{\pi/4} \int_a^{1/\cos\theta} \ln\left(\frac{r}{a}\right) dr\, d\theta}{\ln\left(\frac{\sqrt{\left(\frac{\delta x}{2}\right)^2+\left(\frac{\delta y}{2}\right)^2}}{a}\right)} \frac{\delta z}{\delta x\, \delta y}.\end{aligned} \tag{13}$$

It can be seen from (5) that the value of the conductivity σ requires no modification.

For the special case of a mesh with square cross section $\delta x = \delta y$, the values of the parameters $\varepsilon_x, \varepsilon_y$, etc. will take the value of unity when the radius equals $\delta x \exp(0.5\pi)^{-1} = 0.203\delta x$. This is the radius which would, in fact, be modelled if basic FDTD were used. This "equivalent radius" is lower than the value of $0.23\delta x$ used in [5] and lies between this value and the value of $0.135\delta x$ used in [9]. It is also in agreement with the value of $0.2\delta x$ derived in [10] for a filamentary hard source.

$$\delta y \delta z \left(\frac{\partial}{\partial t} + \frac{\sigma}{\varepsilon}\right) \langle\langle E_x(i+0.5,j,k)\rangle\rangle_{yz} = \frac{1}{\varepsilon}\begin{pmatrix} \delta y \left(\langle H_y(i+0.5,j,k-0.5)\rangle_y - \langle H_y(i+0.5,j,k+0.5)\rangle_y\right) \\ -\delta z \left(\langle H_z(i+0.5,j-0.5,k)\rangle_z - \langle H_z(i+0.5,j+0.5,k)\rangle_z\right)\end{pmatrix} \tag{3}$$

$$\delta y \delta z \frac{\partial}{\partial t} \langle\langle H_x(i,j+0.5,k+0.5)\rangle\rangle_{yz} = \frac{1}{\mu}\begin{pmatrix} \delta y \left(\langle E_y(i,j+0.5,k+1)\rangle_y - \langle E_y(i,j+0.5,k)\rangle_y\right) \\ -\delta z \left(\langle E_z(i,j+1,k+0.5)\rangle_z - \langle E_z(i,j,k+0.5)\rangle_z\right)\end{pmatrix} \tag{4}$$

$$\left(\frac{\partial}{\partial t} + \frac{\sigma}{\varepsilon}\right) \langle E_x\,(i+0.5,j,k)\rangle_x = \frac{1}{\varepsilon\varepsilon_x \delta y \delta z}\begin{pmatrix} \delta y \left(\langle H_y(i+0.5,j,k-0.5)\rangle_y - \langle H_y(i+0.5,j,k+0.5)\rangle_y\right) \\ -\delta z \left(\langle H_z(i+0.5,j-0.5,k)\rangle_z - \langle H_z(i+0.5,j+0.5,k)\rangle_z\right)\end{pmatrix} \tag{5}$$

where

$$\varepsilon_x = \frac{\langle\langle E_x \rangle\rangle_{yz}}{\langle E_x \rangle_x}. \tag{6}$$

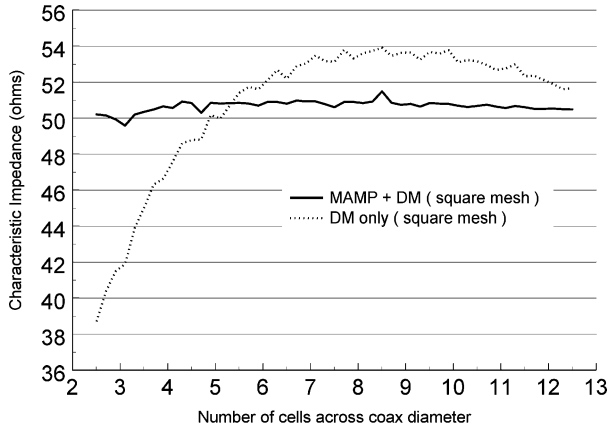

Fig. 2. Calculated characteristic impedance of a coaxial cable using square mesh.

III. Results Obtained Using Analytically Derived MAMPs

A. Lossless Coaxial Lines

The modeling of coaxial lines using FDTD including enhancements which avoid the necessity of a fine mesh, has been addressed in the literature [11]. In that paper, it was shown that good results, even with very coarse meshes, could be obtained by using a thin wire formalism [12] for the center conductor and the Dey–Mittra (DM) locally conformal method [13] for the outer conductor.

Results for a test structure consisting of a 50-Ω line having an inner radius of 0.354 mm, an outer radius of 2.44 mm, and a permittivity of 5.37, as in [11], are shown in Fig. 2. It can be seen that by applying analytical MAMPs to the inner conductor and the DM method to the outer conductor, results are obtained which show a considerable improvement in accuracy compared with the DM method, when used on its own. The ripple which appears on the results has its origin in the DM approximation of the outer conductor in which the error varies nonmonotonically with the exact position of the boundary.

The characteristic impedance is calculated by taking a snapshot of the field distribution in the coaxial line, using Ampere's Law to calculate the current, and the integral of the radial E field to calculate the voltage.

When using MAMPs, the FDTD nodes always store the amplitude of the field component averaged along the cell edge. Thus, the voltage is calculated by summing up the radial E field at the nodes shown in Fig. 3, and multiplying by the cell size. Similarly, the current is found by summing up the values of circumferential H field at the nodes shown in Fig. 4, and multiplying by the cell size.

In this case, the wire formalism of [12] yields formally identical results to the method described here. However, in [12], the correction factors are derived in a less direct and more complicated, two-step manner.

In order to ascertain that the method is effective when the mesh is not of square cross section, the same coaxial cable was analyzed using a 2:1 ratio for the cell size in the two transverse directions. The results show (Fig. 5) considerably greater accuracy than the DM method especially for the coarser meshes. Because of the smaller size of the cell, the method can only be applied for thinner wires. For wires whose radius approaches the size of the smaller side of the cell, the DM method is used.

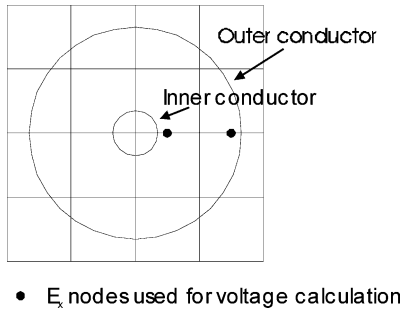

Fig. 3. E nodes used for calculating the voltage.

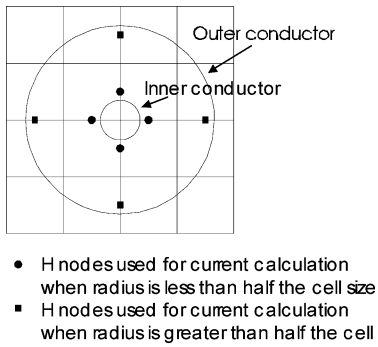

Fig. 4. H nodes used for calculating the current.

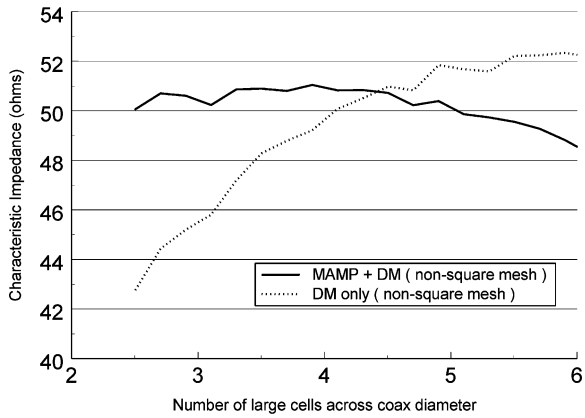

Fig. 5. Calculated characteristic impedance of a 50-Ω coax line using a rectangular mesh.

B. Lossy Coaxial Line

In the literature, there has been significant interest in the modeling of earth grids consisting of electrically thin wires placed in a lossy material, such as soil [5], [14], and [15], for both electromagnetic compatibility (EMC) and safety applications. In [5], the thin wires are modeled using an extended version of the method originally described in [16] and which makes use of the "equivalent radius" concept for thin wires. However, this

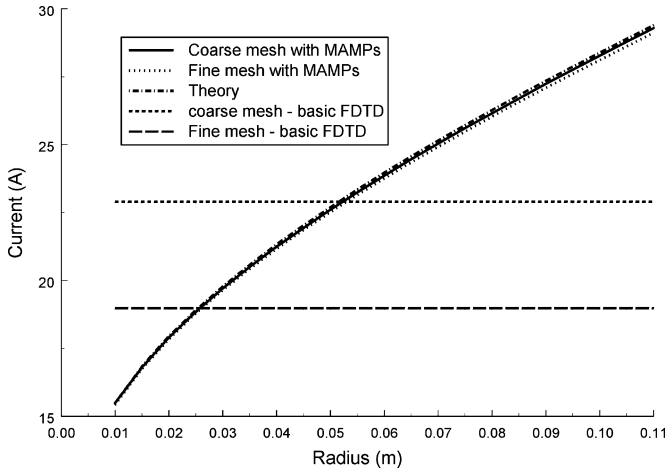

Fig. 6. Steady-state currents conductivity is 5 mS/m.

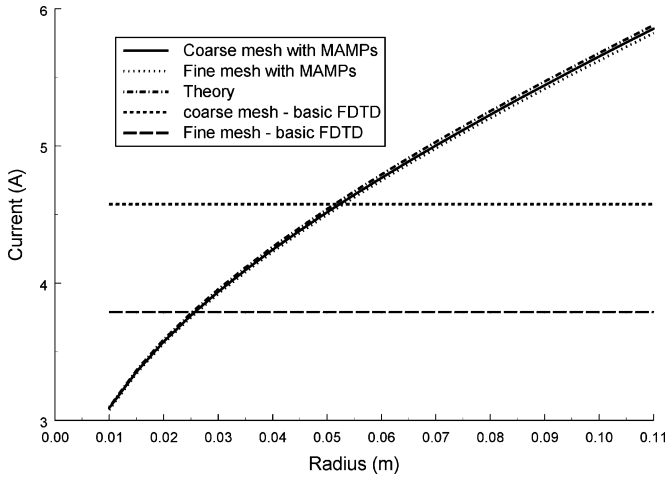

Fig. 7. Steady-state currents conductivity is 1 mS/m.

concept is approximate and is only applicable for square meshes and circularly cylindrical wires and posts.

Since the formulation presented in Section II is based upon the asymptotic field distribution in the vicinity of the wire, the values obtained for the MAMPs are not affected if the dielectric surrounding the wire is lossy as long as the material conductivity is much less than that of the wire. Similarly, if the material is dispersive, the method can still be applied simply by multiplying the time-dependent permittivity and the factors given in (11)–(13). It can, therefore, be applied in an identical way to the problem of lossy coaxial structures. In this section, lossy coaxial transmission lines of 25 m in length, having an outer radius of 1.59 m, filled with a dielectric or relative permittivity of 12 and with conductivities of 1 and 5 mS/m were examined. The line was excited with a 100-V source having a rise time of 20 ns. The structures were modeled using two different FDTD cell sizes, 0.25 and 0.125 m. In each case, the steady-state current was calculated and compared theoretically.

In Figs. 6 and 7, the calculated steady currents using FDTD enhanced with MAMPs are plotted versus the radius of the inner conductor for dielectric conductivities of 5 and 1 mS/m, respectively. Also shown are the theoretical results [17] and the results which are obtained using the basic FDTD. The latter depend only on the cell size, and do not take into account the radius of the conductor. It can be seen that there is agreement between theoretical results and those calculated using MAMPs, both for coarse and fine meshes.

In Fig. 8, the errors in the calculated results are plotted. It can be seen that even for a mesh size of 0.5 m, corresponding to just six cells across the diameter of the coaxial line, results are accurate upto 1.5%. It is noted that the lines representing the results obtained from basic FDTD cross the theoretical curves close to radii of 0.25 and 0.5 m which agrees with the expected "equivalent radius" of $0.203\delta x$ given in Section II.

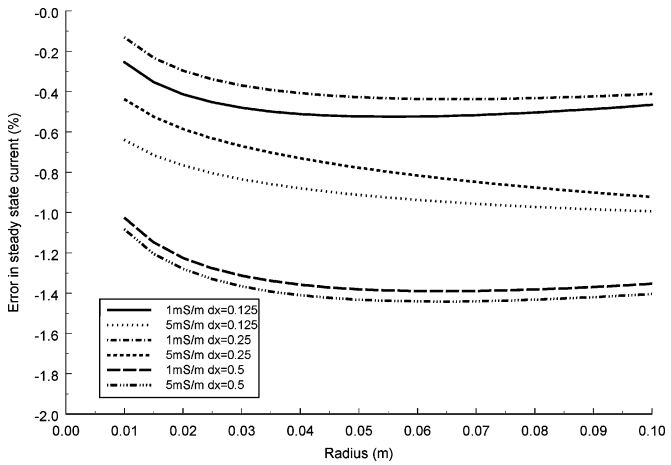

Fig. 8. Errors in calculated steady current for a lossy coaxial line for different inner conductor radii and dielectric conductivities. Outer conductor radius is 1.59 m.

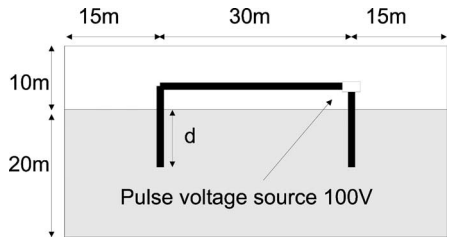

Fig. 9. Earthing rods in soil.

C. Earthing Rods

Another situation, in which the behavior of cylinders in lossy media is important, is the case of earthing rods in soil. An example of this type of structure was examined in [5] using FDTD with an enhancement which is similar, but less flexible and accurate, than the one described here. This structure, which is shown in Fig. 9, was analyzed using the present approach and results compared to those obtained in [5] and the formula given in [17]. The relative permittivity of the soil was taken as 12. Conductivities of 1 and 5 mS/m, immersion depths d of 3 and 5 m, and rod radii of 57.5 and 12 mm were considered. The results

TABLE I
CALCULATED RESISTANCE OF AN EARTHING ROD OF RADIUS 57.5 MM

Immersion depth (m)	3		5	
Conductivity (mS/m)	1	5	1	5
[5]	214	43.2	145	29.3
[17]	230	46.1	154	30.9
MAMP	238	47.7	163	32.7
% disagreement [5] and [17]	7.2	6.5	6.0	5.3
% disagreement MAMP and [17]	3.8	3.5	5.7	5.8

TABLE II
CALCULATED RESISTANCE OF AN EARTHING ROD OF RADIUS 12 MM

Immersion depth (m)	3		5	
Conductivity (mS/m)	1	5	1	5
[17]	313	62.7	204	40.9
MAMP	310	62.0	207	41.6
% disagreement MAMP and [17]	1.0	1.6	1.2	1.7

are summarized in Tables I and II. In each case, the results are compared with those predicted by the widely used formula given in [17] and were available with the results given in [5]. It can be seen that there is, in almost all cases, closer agreement between the MAMP method and [17] than between [5] and [17]. For the z directed rods, the value of ε_x and ε_y were 1.07 for a radius of 57.5 and 0.52 for a radius of 12 mm. The values of μ_x and μ_y were 0.94 for a radius of 57.5 mm and 1.92 for a radius of 12 mm.

D. Stacked Patch Antenna

In order to confirm that the method is equally applicable to wires and coaxial structures which are a part of a complicated structure, the short-stacked patch microwave antenna described in [18] was chosen as an example. This antenna is fed with a coaxial line and also includes a cylindrical shorting post as shown in Fig. 10. The upper patch is 36 mm $\times$ 23 mm, the lower patch is 23 mm $\times$ 23 mm. One shorting post is an extension of the coaxial feed and has a radius of 0.325 mm and is placed 15 mm from the edge of the patches. The other shorting post is placed 1 mm from the edge of the patch and radii between 0.5 and 0.75 mm were considered. The radius of this shorting post has a noticeable influence on the resonant frequency and so, makes a good test for the algorithm. The height of the lower patch above the ground plane is 2 mm and the height of the upper patch is 20 mm.

The antenna was first modeled for several different shorting post radii using basic FDTD with a non-uniform grid, a portion of which is shown in Fig. 11, which was chosen so that the cylinders could be well resolved. The curvature of the outer conductor of the coaxial feed was accounted for by means of the DM algorithm. The simulation was then repeated using a much coarser almost uniform mesh, shown in Fig. 12, which had a cell size of 1 mm and, in this case, MAMPs were included. The required computational time when using the coarse uniform mesh was less than 1/20 of that required when using the finer mesh.

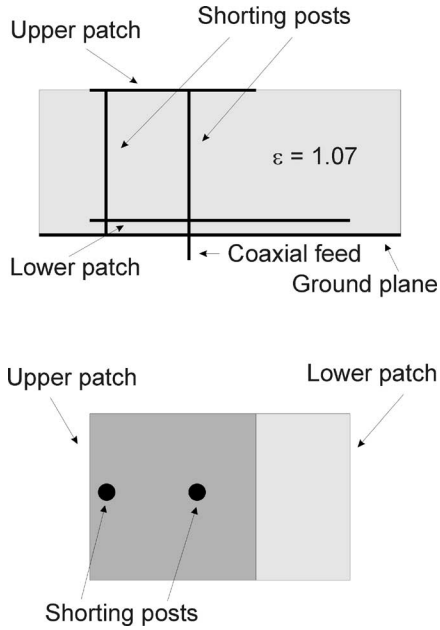

Fig. 10. Elevation and plan view of the shorted stacked patch antenna.

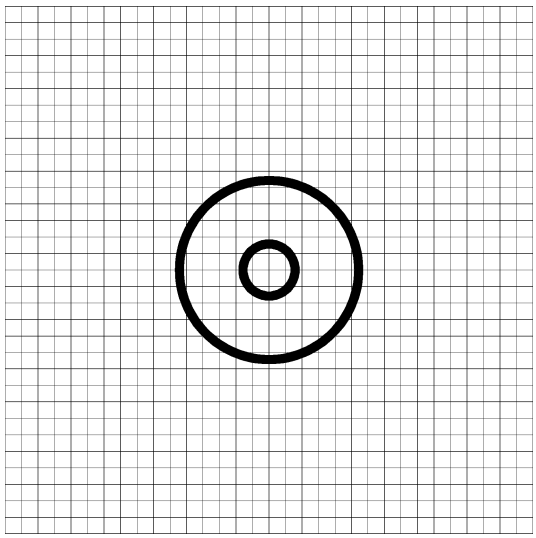

Fig. 11. Fine mesh around coax feed.

The results for shorting post radii of 0.5, 0.6, and 0.75 mm are shown in Figs. 13–15, respectively. Also plotted are the results given by the basic FDTD method which are the same regardless of radius. It can be seen that the position of the resonance frequency of the antenna rises as the radius of the post increases. For the 0.5-mm shorting post, the resonance frequency calculated using the basic coarse mesh is approximately 3% higher when the basic FDTD is used with a fine mesh. When MAMPs are used with the coarse mesh, there is a much better agreement with fine mesh. In the case of the 0.6- and 0.75-mm shorting posts, the use of MAMPs again reduces the discrepancy in predicted resonant frequency between coarse and fine mesh.

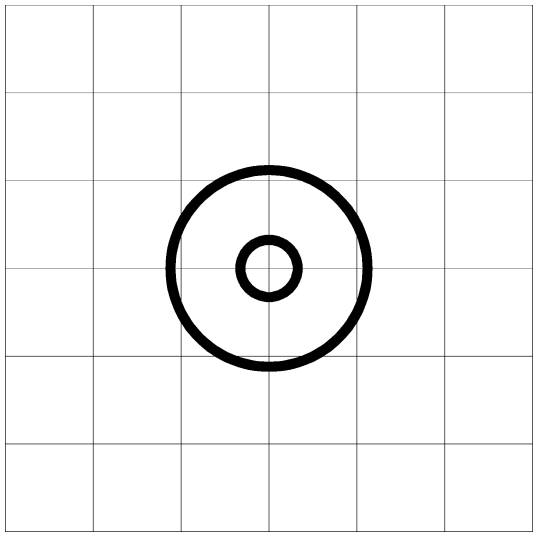

Fig. 12. Coarse mesh around coax feed.

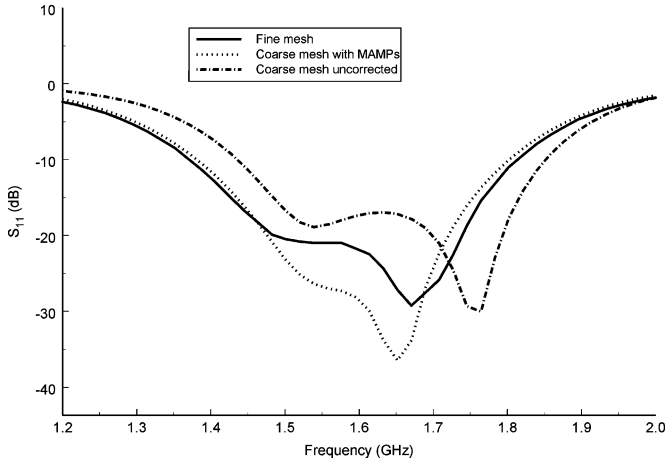

Fig. 13. Calculated return loss of the patch antenna using different methods (post radius 0.5 mm).

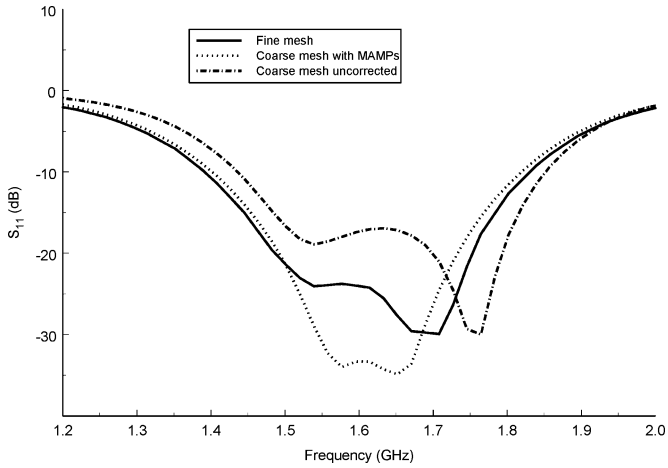

Fig. 14. Calculated return loss of the patch antenna using different methods (post radius 0.6 mm).

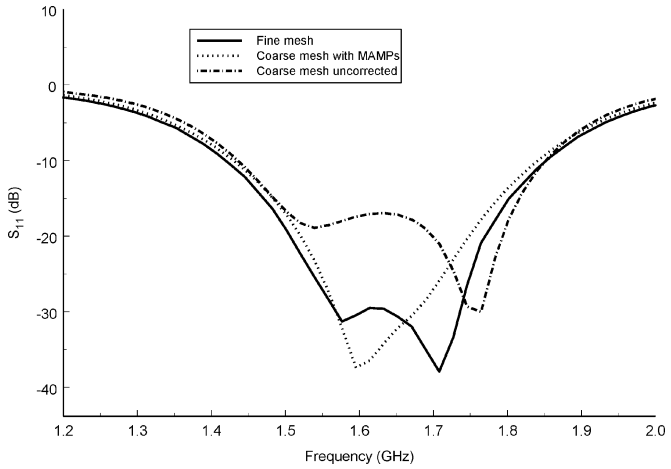

Fig. 15. Calculated return loss of the patch antenna using different methods (post radius 0.75 mm).

IV. Conclusion

In this paper, the use of analytically calculated MAMPs in the FDTD method has been extended to enable them to be applied to wires and coaxial structures, in both lossless and lossy materials. It has been shown that substantial improvements in accuracy can be obtained using this technique for practical situations. This approach has advantages of simplicity, robustness, and versatility over other methods of treating geometrical detail. In particular, the concept of "equivalent radius" is not necessary and the method is readily applied to different metal structures and meshes.

References

[1] C. J. Railton, "The inclusion of fringing capacitance and inductance in FDTD for the robust accurate treatment of material discontinuities," *IEEE Trans. Microw. Theory Tech.*, vol. 48, no. 12, pp. 2283–2288, Jan. 2000.

[2] ——, "The choice of cell size and the use of pre-calculated correction factors in the analysis of planar circuits using FDTD and TLM," in *Proc. Eur. Microw. Conf.*, London, U.K., Sep. 2001, pp. 137–140.

[3] C. J. Railton and D. L. Paul, "Analysis of circular waveguide filter using enhanced FDTD," *Int. J. Numer. Modelling Electron. Netw. Devices Fields*, vol. 15, no. 5–6, pp. 535–547, Sep.–Dec. 2002.

[4] C. J. Railton, D. L. Paul, I. J. Craddock, and G. S. Hilton, "The treatment of geometrically small structures in FDTD by the modification of assigned material parameters," *IEEE Trans. Antennas Propag.*, vol. 53, no. 12, pp. 4129–4136, Dec. 2005.

[5] Y. Baba, N. Nagaoka, and A. Ametani, "Modelling of thin wires in a lossy medium for FDTD simulations," *IEEE Trans. Electromagn. Compat.*, vol. 47, no. 1, pp. 54–60, Feb. 2005.

[6] T. Weiland, "A discretisation method for the solution of Maxwell's equations for six component fields," *Int. J. Electron. Commun. (AEU)*, vol. 31, pp. 116–120, 1977.

[7] T. Weiland, "Time domain electromagnetic field computation with finite difference methods," *Int. J. Numer. Modelling Electron. Netw. Devices Fields*, vol. 9, pp. 259–319, 1996.

[8] R. Holland and L. Simpson, "Finite-Difference analysis of EMP coupling to thin struts and wires," *IEEE Trans. Elecromagn. Compat.*, vol. EMC-23, no. 2, pp. 88–97, May 1981.

[9] K. R. Umashankar, A. Taflove, and B. Becker, "Calculation and experimental validation of induced currents on coupled wires in an arbitrary shaped cavity," *IEEE Trans. Antennas Propag.*, vol. AP-35, no. 11, pp. 1248–1257, Nov. 1987.

[10] G. Waldschmidt and A. Taflove, "The determination of the effective radius of a filamentary source in the FDTD mesh," *IEEE Microw. Guided Wave Lett.*, vol. 10, no. 6, pp. 217–219, Jun. 2000.

[11] D. L. Paul, C. J. Railton, and I. J. Craddock, "Full-wave modelling of coaxial cables by FDTD technique," *Electron. Lett.*, vol. 38, no. 21, pp. 1261–1262, Oct. 2002.
[12] R. M. Makinen, J. S. Juntunen, and M. A. Kivikoski, "An improved thin wire model for FDTD," *IEEE Trans. Microw. Theory Tech.*, vol. 50, no. 5, pp. 1245–1255, May 2002.
[13] S. Dey and R. Mittra, "A locally conformal finite-difference time domain algorithm for modeling three-dimensional perfectly conducting objects," *IEEE Microw. Guided Wave Lett.*, vol. 7, no. 9, pp. 273–275, Sep. 1997.
[14] M. A. da Frota Mattos, "Grounding grids transient simulation," *IEEE Trans. Power Del.*, vol. 20, no. 2, pp. 1370–1378, Apr. 2005.
[15] Y. Liu, N. Theethayi, and R. Thottappillil, "An engineering model for transient analysis of grounding system under lightning strikes: Non-uniform transmission-line approach," *IEEE Trans. Power Del.*, vol. 20, no. 2, pp. 722–730, Apr. 2005.
[16] K. Umashankar, A. Taflove, and B. Beker, "Calculation and experimental validation of induced currents on coupled wires in an arbitrary shaped cavity," *IEEE Trans. Antennas Propag.*, vol. AP-35, no. 11, pp. 1248–1257, Nov. 1987.
[17] E. D. Sunde, *Earth Conduction Effects in Transmisison Systems*, New York: Dover, 1968.
[18] R. B. Waterhouse, "Broadband stacked shorted patch," *Electron. Lett.*, vol. 35, pp. 98–100, 1999.

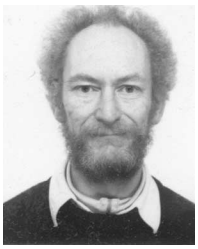

Chris J. Railton received the B.Sc. degree in physics from the University of London, London, U.K., in 1974 and the Ph.D. degree in electronic engineering from the University of Bath, Bath, U.K., in 1988.

During 1974–1984, he worked with the Scientific Civil Service on various research and development projects in the areas of communications, signal processing, and electromagnetic compatibility (EMC). From 1984 to 1987, he was with the University of Bath, working on the mathematical modeling of boxed microstrip circuits. Currently, he is the Head of Computational Electromagnetics Group, Centre for Communications Research, University of Bristol, Bristol, U.K., where he is engaged in the development of new algorithms for electromagnetic analysis and their application to the design of monolithic microwave integrated circuits (MMICs), planar and conformal antennas, microwave and RF heating systems, EMC, high-speed interconnects, and optical waveguide components.

Dominique L. Paul (M'03) received the D.E.A. degree in electronics from Brest University, Brest, France, in June 1986 and the Ph.D. degree from Ecole Nationale Superieure des Telecommunications de Bretagne (LEST-ENSTBr), Brest, in January 1990.

From 1990 to 1994, and from 1995 to 1996, she was a Research Associate at the Centre for Communications Research, University of Bristol, Bristol, U.K., and at the Escuela Tecnica Superior de Ingenieros de Telecomunicacion of Madrid, Spain, under a grant from the Spanish Government, respectively. Since 1997, she has been a Research Fellow at the Centre for Communications Research, University of Bristol, where, since 2003, she has been holding a permanent position. Her research interests include the electromagnetic modeling of passive devices such as microwave heating systems, dielectric structures at millimeter wavelengths, multiple-input multiple-output (MIMO) systems, low profile antennas, and conformal antenna arrays.

Sema Dumanli received the Dipl.-Eng. degree in electrical electronics engineering from Middle East Technical University (METU), Ankara, Turkey, in 2006.

During that period, she spent four months with Computational Electromagnetics Group, Bristol University, Bristol, U.K. Since February 2006, she has been with Aselsan A S, Ankara.